Silicon Micromachined Continuous Inkjet (CIJ) Printhead with Integral Deflection and Guttering

H. V. Panchawagh[1], C. N. Anagnostopoulos[2], A. G. Lopez[1], K. Vaeth[1], G. A. Hawkins[1]; [1]Eastman Kodak Company, Rochester, NY; [2]University of Rhode Island

Abstract

Continuous Inkjet (CIJ) printing technology offers an ideal solution to meet the growing demands of the commercial digital printing market because of its advantages in speed, cost, and reliability. Here we present progress on the development of a new integrated CIJ printhead that can be batch manufactured using standard silicon microfabrication and 3D wafer assembly techniques. The printhead consists of a network of microfluidic channels for drop generation, drop selection, and guttering. The drop generator is a microelectromechanical system (MEMS) fabricated using CMOS-compatible processes. Typical operation of the drop generator involves breakup of a jet stream into small and large drops using thermal stimulation. The drops are then sorted using an air cross-flow, with the small nonprint drops sent to the gutter for recirculation and the large print drops sent to the print media. Laminating individually etched silicon wafers creates the channels for air cross-flow and guttering of the nonprint ink drops. Details on design, fabrication, and characterization of the integrated CIJ printhead are provided, and challenges and future directions are discussed.

Introduction

The trend for many graphics printing applications, such as direct mailings, transactional/promotional documents, catalogues, and magazines, is higher levels of customization and shorter production runs, which is an ideal fit for digital printing technologies. In order to be competitive with the analogue offset printing technology currently used to generate many of these materials, stringent requirements of high image quality and low print cost per page must be met. Continuous inkjet (CIJ) printing technology offers many of the advantages of the low cost and high throughput, however, suffers from disadvantages of lower image quality and limited ink-substrate latitude. Kodak's next generation CIJ technology, KODAK Stream Technology [1], is aimed at overcoming these limitations and meeting the print speed, image quality, and cost requirements of the commercial printing market.

A typical CIJ print engine includes a drop generator, a drop separator to sort print and nonprint drops, and a gutter or a catcher to collect and recirculate the nonprint drops. In conventional CIJ technology [2], ink drops are generated by mechanical stimulation of micrometer scale inkjets using a piezoelectric transducer, the drop selection achieved via inducing charge on the drops, which are then deflected using electrostatic force. Figure 1 shows a schematic of KODAK Stream Technology. Here, the drop generator is a silicon-based microelectromechanical system (MEMS), fabricated with integrated CMOS drivers and associated circuitry [3-5]. Typical operation of the printhead involves generation of small and large drops of fluid via jet breakup controlled by low-energy pulses applied periodically to a heater situated around each jet orifice [6]. The drops are then sorted using an air cross-flow, with the small nonprint drops sent to the gutter for recirculation, and the large print drops are sent to the print media [7]. The printhead is stationary in this system, with the print media moving underneath at speeds of hundreds of feet per minute. The main advantages of this technology are high printing speed, low cost per page, high image quality, ability to run relatively large printing jobs without requiring cleaning or other maintenance, and its potential for printing a wide range of materials.

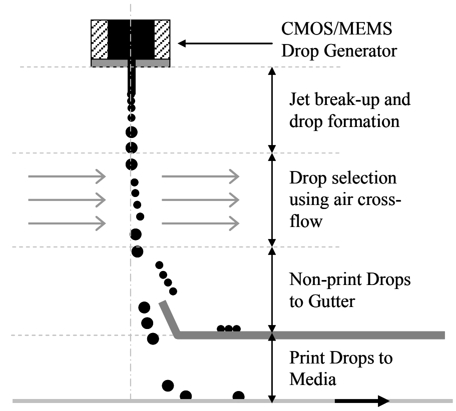

Figure 1. Schematic illustrating KODAK Stream Technology [1].

In this paper, we present a method for precision batch fabrication of compact, integrated CIJ printheads using silicon microfabrication and wafer bonding techniques [8]. This method is illustrated by building and testing of a miniaturized printhead based on the scheme shown in Figure 1, where all of the functionalities of a CIJ print engine are integrated into a monolithic microfluidic device.

Design

At the heart of the printhead is a silicon micromachined drop generator that creates continuous streams of ink drops via thermal stimulation. Figure 2 shows the cross-sectional view of a single nozzle. It is formed on a 300 µm thick silicon wafer coated with a dielectric film stack that acts as a nozzle membrane (2.1 µm thick) with a circular orifice (8.0 µm diameter). Ink is supplied to the orifice via an ink feed channel (30 µm × 120 µm) etched in the silicon wafer. Concentric resistive heater elements (inside diameter 10 µm, outer diameter 14 µm, thickness 0.19 µm, calculated resistance 830 Ω) are embedded around each of the nozzle orifices for jet stimulation. A nozzle orifice of D = 8 µm diameter is selected to give small and large drop volumes of 1.8 pL (1X) and 7.2 pL (4X), respectively, for the typical value of $\lambda/D = 4.5$ for 1X drops, where λ is the wavelength of the jet corresponding to drop generation [6]. For a jet velocity of 20 m/s, a 1X drop generation rate of 555 kHz and 4X drop generation rate of 138 kHz (maximum printing frequency) were calculated.

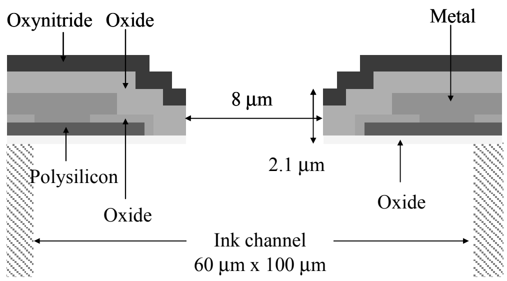

Figure 2. Cross-sectional view of the drop generator showing critical dimensions.

Figure 3 shows the design of the integrated printhead formed by an assembly of five individually etched silicon wafers in addition to the drop generator. The drop generator is located at the top and includes an array of nozzles at a pitch of 84.66 µm corresponding to 300 NPI. The ink drops travel from top to bottom through a narrow channel in the center. This channel hereafter is referred to as the central channel and has a width of about 300 µm, which is more than 10 times the diameter of the large drops. A uniform cross-flow of air from left to right deflects the nonprint drops toward a catcher on the right-hand side. This collected ink is then recycled back to the ink supply tank. The physical dimensions of the first prototype device shown in Figure 3 are 3.2 mm in thickness, 10 mm in width, and 45 mm long. The length of the various microchannels that run along the length of the device is 30 mm.

As shown in Figure 3a several rows of through-holes are provided in the drop generator wafer in addition to the ink feed channels to serve as fluidic ports for airflow and ink recirculation. The drop generator wafer is bonded to two 650 µm thick silicon wafers, Spacer1 and Spacer2 (Figure 3b). A channel created in the Spacer1 connecting to the central channel is intended to provide a vent or a collinear air supply with the drop streams. Other long rectangular slots in the spacer wafers provide fluidic interconnections to the subsequent wafers. This spacer wafer stack (Spacer1 and Spacer2) is 1350 µm thick and is designed to allow the jet to break up and form drops of desired size (1X and 4X) before the cross-flow of air deflects them. The next wafer, Air Channel (650 µm thick), forms the channels to provide cross airflow for droplet deflection. This wafer consists of partially and through-etched structures that form deflection channels of 400 µm or 650 µm in height. Another 650 µm silicon wafer, Spacer3, is used to increase the separation of the deflected drops before the nonprint (small or 1X) drops are caught in the gutter. This wafer consists of a notch near the catcher for guttering small drops. The final wafer in the stack, the Gutter wafer, is 300 µm thick and includes a thin vertical knife-edge (width 10 µm, height 150 µm) located at 130 µm from undeflected drop streams. The knife-edge is connected to a 150 µm channel for guttering ink and recirculating it back to the supply tank. A custom steel manifold designed for packaging the printhead is shown in Figure 3c and is used to make electrical and fluidic connections for characterization.

The deflection of the traveling drops in a cross-flow of air was estimated using Newtonian particle mechanics and equations of the fluid drag on the spherical objects. For the prototype geometry, air velocities on the order of 40 m/s were calculated for sorting the print and nonprint drops, which corresponded to airflow rates of 30 L/min.

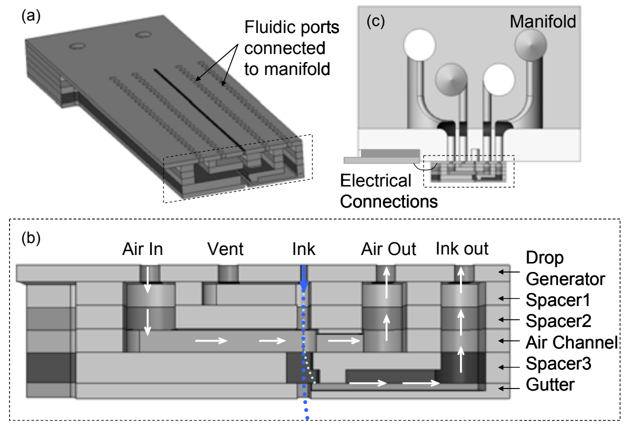

Figure 3. Schematic design of the integrated CIJ printhead. (a) 3D view of a printhead showing wafer stack and fluidic ports; (b) detailed cross-sectional view of the device showing microchannel network formed by laminated wafer stack; and (c) cross-section of the packaged device on a manifold.

Fabrication

The drop generator was fabricated with the standard surface micromachining processes and ink feed channels were etched in silicon by the deep anisotropic reactive ion etch (DRIE) process [9]. All other wafers (Spacer1-Gutter) were also etched using the same process. Channels were appropriately rounded in the mask design to avoid stress concentration and wafer breakage. Wafers Air Channel, Spacer 3, and Gutter were etched in two steps with an oxide hard mask and a soft photoresist mask to create the desired geometry.

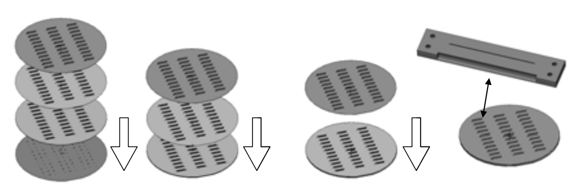

Figure 4. Illustration of batch fabrication process of the integrated printhead using wafer bonding.

The wafers were aligned optically using photolithographically defined targets and bonded together using a thin (~ 0.3 µm) layer of adhesive [10]. See Figure 4. The bonding pressure used was 30 psi and the maximum temperature used for curing of the adhesive was below 200 °C. Thus, the wafer bonding process was CMOS-compatible. After the bonding step, the wafer stack was cut into individual devices using a dicing saw.

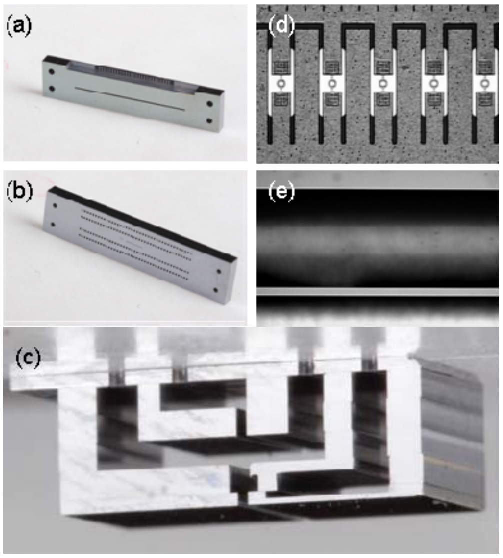

Figure 5. Integrated printhead after fabrication. (a) and (b) show the view of the complete device from two sides; (c) shows the device cross-section; (d) shows the front face of the drop generator; and (e) shows the vertical knife edge catcher.

Devices with different wafer stacks, namely, those including (i) Drop Generator, Spacer1 and Spacer2, (ii) Drop Generator, Spacer1, Spacer2, Air Channel, and Spacer3, and (iii) complete five wafer stack were built. Figure 5 shows images of a completed printhead after the dicing step. The front-view of the device showing the central channel opening in the Gutter wafer through which the print drops are ejected is shown in Figure 5a. This view also shows an opening in the wafer stack around the bond pads for electrical connections. Four rows of through-holes for various fluidic ports are visible in Figure 5b. The ink feed channels were etched only for the 48 nozzles in the middle for testing. A cross-sectional view of the device is shown in Figure 5c and reveals a good alignment between wafers. Generally, alignment accuracy on the order of 10 μm was achieved between the nozzle array and knife-edge catcher. Figure 5d shows a frontside view of the nozzles with ring heaters, metal connections, and ink feed channels illuminated with backside lighting. Figure 5(e) shows the silicon knife-edge formed by the two-step DRIE process.

Experimental

The singulated printheads were attached to manifolds using an epoxy. Circular holes provided in wafer stack (Figure 5a) were used for alignment of the fluidic ports in the wafer stack with the manifold channels. Electrical connections were made to an external flexible circuit via wire-bonding. A pressurized vessel was used to supply fluid to the drop generator. The aqueous test fluid used in the experiments had a density, viscosity, and a surface tension of 1 g/mL, 0.92 cP, and 0.42 dynes/cm, respectively. Typically, the heat pulses are controlled by on-chip CMOS circuitry. However, as the initial prototype drop generator had no integrated CMOS circuitry, external signal generators were used. For initial testing, three banks of 16 heaters each connected in parallel configuration were driven with three separate synchronized signal generators. Air blowers were used for providing deflection air with in-line flow meters. The drop streams exiting the printhead were imaged using a CCD camera with a magnifying lens and LED strobe light.

Results and Discussion

First, it was ensured that 1X and 4X drops were formed before they reached the air deflection channel by looking at drops exiting from the stack (i). For drop velocities on the order of 20 m/s and fundamental (1X) frequency 555 kHz, 1X and 4X drops were reliably formed by using customized waveforms for heater voltages of 3 to 4 V or energy per 1X drop on the order of 10 nJ. See Figure 6a. The complete stack (iii) was also tested without airflow to demonstrate drop ejection through the long and narrow central channel (Figure 6b). This experiment revealed a potential issue with the printhead due to excess drag on the small drops as they travelled through the central channel. This drag resulted in the coalescing of successive small drops. This can result in insufficient separation between print and nonprint drops for guttering. This problem will be addressed in future designs by increasing the width of the central channel.

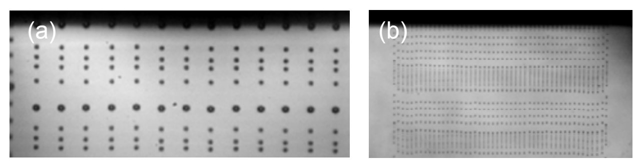

Figure 6. (a) Front view showing large and small drops formed as they travel through the Spacer1-Spacer2 stack; (b) drops ejecting through complete device stack.

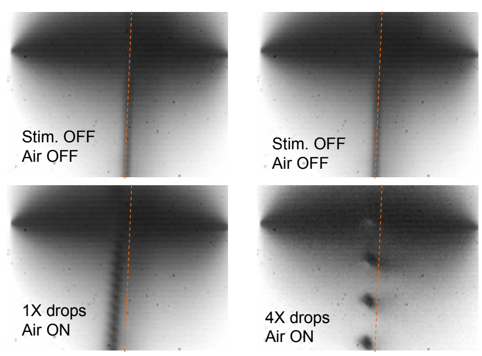

Figure 7. Example of small and large deflection using airflow in the integrated printhead (side view).

Assembly (ii) was used to study drop deflection with cross airflow. As shown in Figure 7, even for small airflows, both the small and large drops were deflected when airflow was turned on. The small drops were deflected more compared to the large drops, as expected. Figure 8 shows an illustration of integrated deflection and guttering with the complete printhead for two different combinations of 1X and 4X drops. When airflow was turned on, the nonprint drops were deflected into the gutter and print drops were ejected towards media. The airflow conditions for this experiment were positive airflow (left of main channel) of 16 L/min, negative airflow (right of air channel) of 12 L/min and gutter channels of 6 L/min.

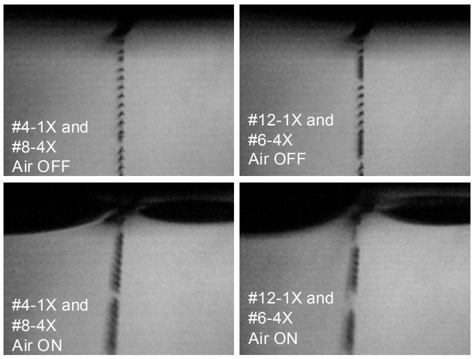

Figure 7. Illustration of deflection and guttering using airflow in the integrated printhead (side view).

Note that in Figure 7 the print drops look "fuzzy" as they exit the printhead. This was caused by positional variations in the successive drops resulting from turbulence at high airflow rates. This is clear from the noticeable angular deflection of the print drops from the undeflected position. These higher airflow rates were required because of the compact design of the prototype. Further, there was a tendency of additional merging of successive small drops with airflow as some air was entrained from the bottom opening in the central channel, causing adverse drag on the drops. These issues can be addressed by redesigning the printhead to increase drop deflection by optimizing the deflection channel height, adding another spacer wafer before the gutter, and increasing the height of the positive deflection channel. Another issue with the present design was related to formation of an ink puddle at the bottom of the gutter surface, as seen in Figure 7. The current design required very accurate trajectories of the nonprint drops to be effectively caught in the knife-edge gutter. Small deviations in the drop trajectories caused the drops to land on an undesired surface and then created an ink film on the central channel wall and a puddle on the gutter surface. This also caused misting as the drops hit the ink puddle. In future designs this will be addressed by a better catcher design that allows for deviations in small drop trajectories and schemes to siphon any ink that may create a puddle.

Conclusions

In summary, a micromachined, compact, integrated printhead for continuous inkjet printing was proposed. This method offers advantages of batch-fabrication, precision alignment, cleanliness, and potential of adding multiple aligned rows of nozzles in a single printhead. Prototypes were fabricated and were used to demonstrate successful generation of ink drops, selection of print and nonprint drops, and guttering of the nonprint drops. The important issues with the printhead architecture were identified and solutions were suggested. Although the device was demonstrated for using air deflection, this concept can be applied for any continuous inkjet printing scheme including electrostatic deflection and thermal deflection [2-4].

Acknowledgments

The authors gratefully acknowledge contributions of the staff at the microfabrication and micropackaging laboratory at Kodak Research Laboratories as well as Almon Fisher and Dr. Nancy Stoffel of Infotonics in building device prototypes.

References

[1] G.A. Hawkins, J. M. Chwalek, C. N. Delametter, E. P. Furlani, D. L. Jeanmaire, J. A. Lebens, D. P. Trauernicht, and Q, Yang, Application of Instabilities in Microfluidic Jets to Digital Offset-Class Printing, Hilton Head Workshop 2008: A Solid-State Sensors, Actuators and Microsystems Workshop, Hilton Head Island, SC, June 1-5, 2008.

[2] H. P. Le, Progress and Trends in Ink-jet Printing Technology, Journal of Imaging Science and Technology, 42 (1), January/February 1998.

[3] C. N. Anagnostopoulos, J. A. Lebens, D. P. Trauernicht, J. M. Chwalek, and C. N. Delametter, CMOS/MEMS Integrated Ink Jet Print Head and Method of Forming Same, US 2003/0016272 A1, Eastman Kodak Company, Sep 2002.

[4] J. M. Chwalek, D. P. Trauernicht, C. N. Delametter, R. Sharma, D. L. Jeanmaire, C. N. Anagnostopoulos, G. A. Hawkins, B. Ambravaneswaran, J. C. Panditaratne, and O. A. Basaran, A New Method for Deflecting Liquid Microjets, Phys. Fluids 14, L37, 2002.

[5] C. N. Anagnostopoulos, J. M. Chwalek, C. N. Delametter, G. A. Hawkins, D. L. Jeanmaire, J. A. Lebens, A. G. Lopez, and D. P. Trauernicht, Micro-Jet Nozzle Array for Precise Droplet Metering and Steering Having Increased Droplet Deflection, Proc IEEE, Transducers 2003, Boston, 368-71, June 8-12, 2003.

[6] E. P. Furlani, Temporal Instability of Viscous Liquid Microjets with Spatially Varying Surface Tension, J. Phys. A: Math. Gen. 38, 263-276, 2005.

[7] D. L. Jeanmaire and J. M. Chwalek, Printhead Having Gas Flow Ink Droplet Separation and Method of Diverging Ink Droplets, US 2002/0122102 A1, Eastman Kodak Company, Dec 2000.

[8] M.A. Schmidt, Wafer-to-Wafer Bonding for Microstructure Formation, Proc IEEE, 86 (8), 1575-1585, Aug 1998.

[9] F. Laerme, A. Schilp, K. Funk, and M. Offenberg, Bosch Deep Silicon Etching: Improving Uniformity and Etch Rate for Advanced MEMS Applications, Proc IEEE, MEMS'99, 211-216, 17-21 Jan 1999.

[10] N. Stoffel, A. Fisher, T. Songsheng M. Boysel, J.W. Grover, and R. Juncosa, Wafer Level Assembly Methods for Complex Pathway Micro-Fluidic PCR Reactor, Proc Electron Comp Tech Conf, ECTC '07, 1561-1566, May 29 2007-June 1 2007.

Biographies

Hrishikesh V. Panchawagh received his Ph. D. in mechanical engineering from the University of Colorado at Boulder in 2005. His area of expertise includes design, modeling, fabrication, packaging, and testing of MEMS and microfluidics for engineering and biomedical applications. Since 2006 Hrishikesh has worked as a MEMS Research Scientist at Eastman Kodak Company, Rochester, NY, USA. His current research focus is the development of new MEMS and microfluidic devices for inkjet printing applications.

Constantine Anagnostopoulos is an adjunct Full Professor of Mechanical Engineering at the University of Rhode Island. He retired from Eastman Kodak Company in August 2007. He has 70 patents issued mostly in the areas of CCD image sensors and inkjet printheads. In 2005 he was named Distinguished Elite Inventor of Eastman Kodak Company. Dr. Anagnostopoulos has published over 50 papers in conferences and journals. He has served as guest editor of the IEEE transactions on

Electron Devices and the IEEE Journal of Solid State Circuits, and as associate editor of the latter. In 1999 Prof. Anagnostopoulos was elected Fellow of IEEE for his contributions to CCD image sensors and integrated circuits for digital cameras.

Ali G. Lopez received M.S. and Ph.D. degrees in Electrical Engineering from Cornell University and an M.S. degree in Optics from the University of Rochester. His areas of expertise are photonics, integrated optics, MEMS/NEMS technologies, and CMOS/MEMS integration. He has also contributed to the optical design of state-of-the-art digital imaging systems and novel inkjet printhead designs.

Kathleen Vaeth received her B.S. in Chemical Engineering from Cornell University (1994), and her M.S. and Ph.D. in Chemical Engineering from MIT (1999), where she was a Hertz Fellow. She joined Research Laboratories at Eastman Kodak in Rochester, NY in 1999, and has worked in the areas of inkjet drop generator design, fabrication, and characterization, OLED displays, flexible displays, and photothermographic X-ray film. She is also an adjunct faculty member in the Chemical Engineering Department at Cornell University.

Gilbert A. Hawkins received the B.S. and Ph.D. degrees in Physics from Stanford University and MIT, in 1969 and 1973, respectively, and was Miller Fellow of Basic Research at the University of California at Berkeley before joining the Research Labs of the Eastman Kodak Company in 1976. His work at Kodak has focused on imaging systems, CCD sensors, semiconductor processing, and MEMS/NEMS technology development for micro-optical and microfluidic arrays. He has published over 60 technical papers, holds 110 US Patents in those fields, and has participated in the activities of many outside organizations including NSF. He established the Integrated Materials and Microstructures Laboratory at Kodak in 1997 and was Associate Director of Research, Kodak Research Labs until his retirement in 2009.